Journal of Dental Research
2018, Vol. 97(4) 432–441

DOI: 10.1177/0022034517744773
journals.sagepub.com/home/jdr

Hypercementosis Associated with *ENPP1* Mutations and GACI

V. Thumbigere-Math[1,2], A. Alqadi[3], N.I. Chalmers[4], M.B. Chavez[5], E.Y. Chu[1], M.T. Collins[6], C.R. Ferreira[7,8], K. FitzGerald[3,9], R.I. Gafni[6], W.A. Gahl[7], K.S. Hsu[7], M.S. Ramnitz[6], M.J. Somerman[1], S.G. Ziegler[10], and B.L. Foster[5]

Abstract

Mineralization of bones and teeth is tightly regulated by levels of extracellular inorganic phosphate (P_i) and pyrophosphate (PP_i). Three regulators that control pericellular concentrations of P_i and PP_i include tissue-nonspecific alkaline phosphatase (TNAP), progressive ankylosis protein (ANK), and ectonucleotide pyrophosphatase/phosphodiesterase 1 (ENPP1). Inactivation of these factors results in mineralization disorders affecting teeth and their supporting structures. This study for the first time analyzed the effect of decreased PP_i on dental development in individuals with generalized arterial calcification of infancy (GACI) due to loss-of-function mutations in the *ENPP1* gene. Four of the 5 subjects reported a history of infraocclusion, overretained primary teeth, ankylosis, and/or slow orthodontic tooth movement, suggesting altered mineral metabolism contributing to disrupted tooth movement and exfoliation. All subjects had radiographic evidence of unusually protruding cervical root morphology in primary and/or secondary dentitions. High-resolution micro–computed tomography (micro-CT) analyses of extracted primary teeth from 3 GACI subjects revealed 4-fold increased cervical cementum thickness ($P = 0.00007$) and a 23% increase in cementum density ($P = 0.009$) compared to age-matched healthy control teeth. There were no differences in enamel and dentin densities between GACI and control teeth. Histology revealed dramatically expanded cervical cementum in GACI teeth, including cementocyte-like cells and unusual patterns of cementum resorption and repair. Micro-CT analysis of *Enpp1* mutant mouse molars revealed 4-fold increased acellular cementum thickness ($P = 0.002$) and 5-fold increased cementum volume ($P = 0.002$), with no changes in enamel or dentin. Immunohistochemistry identified elevated ENPP1 expression in cementoblasts of human and mouse control teeth. Collectively, these findings reveal a novel dental phenotype in GACI and identify *ENPP1* genetic mutations associated with hypercementosis. The sensitivity of cementum to reduced PP_i levels in both human and mouse teeth establishes this as a well-conserved and fundamental biological process directing cementogenesis across species (ClinicalTrials.gov NCT00369421).

Keywords: cementum, mineralized tissue/development, tooth development, enamel, generalized arterial calcification of infancy, periodontal tissues/development

[1]National Institute of Arthritis and Musculoskeletal and Skin Diseases (NIAMS), National Institutes of Health (NIH), Bethesda, MD, USA
[2]Division of Periodontics, School of Dentistry, University of Maryland, Baltimore, MD, USA
[3]Division of Public and Child Dental Health, Dublin Dental University Hospital, Dublin, Ireland
[4]Analytics and Publication, DentaQuest Institute, Westborough, MA, USA
[5]Division of Biosciences, College of Dentistry, The Ohio State University, Columbus, OH, USA
[6]Section on Skeletal Disorders and Mineral Homeostasis, National Institute of Dental and Craniofacial Research (NIDCR), National Institutes of Health (NIH), Bethesda, MD, USA
[7]National Human Genome Research Institute (NHGRI), National Institutes of Health (NIH), Bethesda, MD, USA
[8]Division of Genetics and Metabolism, Children's National Health System, Washington, DC, USA
[9]Our Lady's Children's Hospital, Crumlin, Dublin, Ireland
[10]Institute of Genetic Medicine, Johns Hopkins University School of Medicine, Baltimore, MD, USA

A supplemental appendix to this article is available online.

Corresponding Author:
B.L. Foster, Division of Biosciences, College of Dentistry, The Ohio State University, 4163 Postle Hall, 305 W. 12th Avenue, Columbus, OH 43210, USA.
Email: foster.1004@osu.edu

Introduction

Bone and tooth mineralization is regulated by extracellular levels of inorganic phosphate (P_i) and pyrophosphate (PP_i). Regulators of pericellular P_i and PP_i concentrations include tissue-nonspecific alkaline phosphatase (*ALPL* gene; TNAP protein), which promotes mineralization by hydrolyzing PP_i, an inhibitor of mineralization; progressive ankylosis protein (*ANKH;* ANK), which mediates intracellular to extracellular PP_i transport; and ectonucleotide pyrophosphatase/phosphodiesterase 1 (*ENPP1;* ENPP1), which converts adenosine triphosphate (ATP) into adenosine monophosphate (AMP) and PP_i (Millán 2013). Inactivating *ENPP1* mutations are associated with generalized arterial calcification of infancy (GACI or GACI1; OMIM#208000), a rare autosomal recessive disorder characterized by prenatal-onset vascular calcification (Rutsch et al. 2003; Ferreira et al. 2014). Bisphosphonates, synthetic nonhydrolyzable PP_i analogues, are the current standard of care to prevent vascular calcifications and improve survival beyond infancy. Some GACI patients surviving past the first year of life develop fibroblast growth factor 23 (FGF23)–mediated hypophosphatemic rickets (ARHR2; OMIM#613312) (Levy-Litan et al. 2010; Lorenz-Depiereux et al. 2010).

Dentoalveolar mineralized tissues (i.e., enamel, dentin, cementum, and alveolar bone) are affected by metabolic disorders of mineralization (Opsahl Vital et al. 2012; Foster, Nociti, and Somerman 2014; Foster, Ramnitz, et al. 2014). Cementum that covers the root surface and anchors the periodontal ligament (Foster and Somerman 2012) is very sensitive to disturbances in the P_i/PP_i ratio. *ALPL* loss-of-function mutations cause increased PP_i concentrations and hypophosphatasia (HPP; OMIM#241500/241510/146300), characterized by skeletal and dental hypomineralization, including inhibition of acellular cementum formation (Reibel et al. 2009; Foster, Ramnitz, et al. 2014). Conversely, genetic ablation of *Ank* or *Enpp1* in mice results in decreased PP_i and increased cementogenesis (Nociti et al. 2002; Foster et al. 2012). However, effects of low PP_i levels on human dentoalveolar development have never been reported. This study for the first time reports the novel dental phenotype associated with biallelic inactivating *ENPP1* mutations in human subjects with GACI. Manifestations are described in 5 subjects and *Enpp1* mutant mice.

Methods and Materials

Human Subjects

Dental and medical findings from 5 GACI patients are reported. Patients were enrolled in National Human Genome Research Institute protocol 76-HG-0238 (ClinicalTrials.gov identifier: NCT00369421) and National Institute of Dental and Craniofacial Research protocol 01-D-0184. Written informed consent was obtained from study participants or legal guardians according to guidelines of the Declaration of Helsinki.

Clinical Examination

All subjects underwent dental examination, including digital panoramic and/or periapical X-rays. Blood studies were completed as part of their medical evaluation. Exfoliated or extracted primary teeth were collected from 3 GACI subjects (10 teeth) and 4 age-matched healthy control subjects (6 teeth) for radiographic and histological analyses (Appendix Table 1). Additional methods for analyzing FGF23, PP_i, and ENPP1 enzyme activity are reported in the Appendix.

Mice

Enpp1 mutant ($Enpp1^{asj/asj}$) and wild-type (WT) mice (12 wk old, $n = 4$ to 5/genotype, including males and females; Jackson Labs C57BL/6J-$Enpp1^{asj}$/GrsrJ) were analyzed. Previous publications describe characterization of $Enpp1^{asj/asj}$ mice (Li et al. 2013). Animal studies were approved by the National Institute of Arthritis and Musculoskeletal and Skin Diseases Animal Care and Use Committee.

Micro–Computed Tomography

Micro–computed tomography (CT) was used to analyze human and mouse teeth. Samples were scanned in a μCT 50 (Scanco Medical) at 70 kVp, 76 μA, 0.5 Al filter, with 900-ms integration and 10-μm voxel dimension for human samples and 1,200-ms integration and 2-μm voxel dimension for mouse samples. Reconstructed images were analyzed using AnalyzePro 1.0 (AnalyzeDirect). Detailed methods for micro-CT analysis are described in the Appendix and Appendix Figure 1.

Histology

Human and mouse teeth were demineralized in an acetic acid/formalin/sodium chloride solution, paraffin embedded, sectioned at 6 μm, and stained with hematoxylin and eosin (H&E) or picrosirius red (Foster 2012). Tartrate-resistant acid phosphatase (TRAP) staining for osteoclast/odontoclast-like cells was performed as previously described (Foster et al. 2017). Immuno-histochemistry (IHC) was performed using a peroxidase-based kit with 3-amino-9-ethylcarbazole substrate (Vector Labs). Use of a polyclonal anti-human ENPP1 antibody (Abcam) was previously described (Zweifler et al. 2015).

Statistical Analysis

Data were analyzed by 2-tailed Student's *t* test with Benjamini-Hochberg false discovery rate correction for $Q = 0.05$ (Prism 7.02; GraphPad Software). Data are expressed as mean ± standard deviation. Additional statistical procedures are described in the Appendix.

Results

Case Descriptions

Case 1. A 6.7-y-old Caucasian female (subject 1) with a history of GACI presented with biallelic *ENPP1* mutations (NM_006208.2: c.913C>A/p.P305T in exon 8; c.1499A>C/p.H500P in exon 15) (Fig. 1A). She is the youngest of 4 children born to healthy nonconsanguineous parents, with 2 healthy older siblings and no family history of coronary artery disease

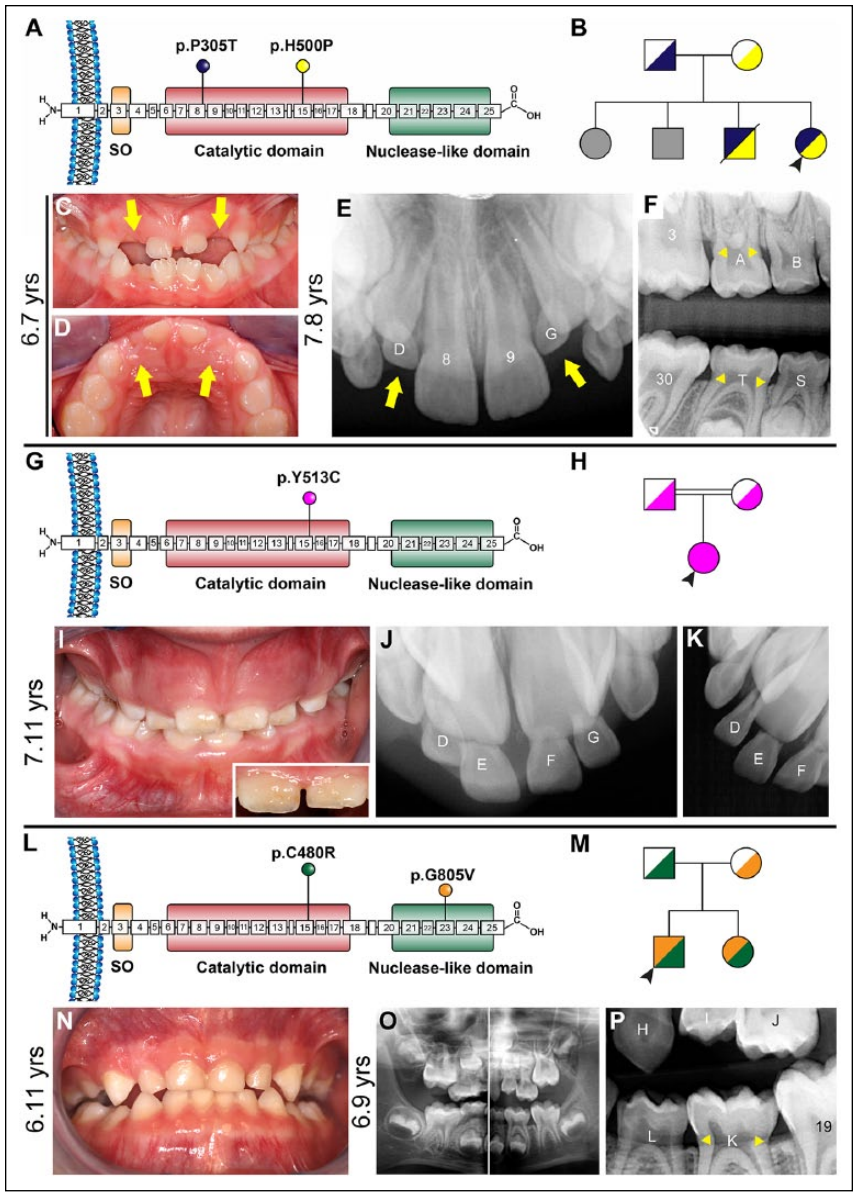

Figure 1. Clinical presentations of generalized arterial calcification of infancy (GACI) subjects 1 to 3. (**A**) Schematic of ENPP1 protein indicating locations of p.P305T (exon 8) and p.H500P (exon 15) amino acid substitutions identified in subject 1. (**B**) Pedigree of proband subject 1 (black arrowhead) showing unaffected parents, 2 unaffected older siblings (unknown genetic composition indicated by gray shading), and an older brother harboring the same biallelic *ENPP1* mutations who died of cardiac arrest. (**C, D**) Clinical photographs at 6.7 y of age reveal infraoccluded primary maxillary lateral incisors (yellow arrows). (**E**) Periapical radiograph at 7.8 y shows eruption of permanent maxillary incisors (8, 9) while primary lateral incisors remain infraoccluded (yellow arrows) and secondary lateral incisors are unerupted. (**F**) Bitewing radiograph reveals a protruding cervical root morphology (yellow arrowheads) in primary and secondary molars, where cementum sometimes appears to overlap enamel at the cementum-enamel junction. (**G**) Schematic of ENPP1 protein indicating the location of the homozygous p.Y513C amino acid substitution in exon 15 identified in subject 2. (**H**) Pedigree of proband subject 2 (black arrowhead) showing unaffected consanguineous parents. (**I**) Clinical photograph of subject 2 at 7.11 y reveals a mixed dentition with gingival hyperplasia and mild discoloration in enamel of central incisors (inset). (**J, K**) Dental radiographs indicate overretained maxillary central and lateral incisors. (**L**) Schematic of ENPP1 protein indicating locations of p.C480R (exon 15) and p.G805V (exon 23) amino acid substitutions identified in GACI subject 3. (**M**) Pedigree of proband subject 3 (black arrowhead) showing unaffected parents and younger sister with GACI. (**N**) Oral photograph at 6.11 y and (**O**) panoramic radiograph at 6.9 y reveal a healthy mixed dentition. (**P**) Dental bitewing radiograph shows protruding cervical root morphology on primary molar K.

(Fig. 1B). A brother carrying the same *ENPP1* mutations died at 4 mo of age due to heart failure secondary to GACI. As part of GACI management, she was treated with bisphosphonates for the first 2 y of life. She was later diagnosed with FGF23-mediated hypophosphatemic rickets (Appendix Table 2). Her detailed medical history is summarized in the Appendix and Appendix Figure 2A–D.

Her dental history was unremarkable for the first 2 y. Her parents noted gradual disappearance of maxillary lateral incisors (D, G) from age 2 through 6 y (Appendix Fig. 4A–C). She was evaluated for this progressive, severe infraocclusion. Oral examination revealed a normally developing mixed dentition, apart from clinically absent maxillary primary lateral incisors and mild to moderate infraocclusion of a mandibular primary first molar (L) (Fig. 1C, D; Appendix Fig. 4D–H). More than a year later (age 7.8 y), maxillary primary lateral incisors remained infraoccluded and permanent successors were unerupted (Fig. 1E). Radiographically, there were 2 notable findings: maxillary primary lateral incisor crowns were completely infraoccluded (Fig. 1E), and primary molars exhibited an unusually protruding morphology in the cervical root (Fig. 1F). Maxillary primary lateral incisors and primary canines (C, D, G, H) were extracted to provide an eruption pathway for permanent incisors. Several months later, permanent incisors were erupted, although infraocclusion of mandibular primary first molar persisted (Appendix Fig. 4I–K). No dental signs of hypophosphatemic rickets (e.g., hypoplastic or discolored enamel, thin dentin, prevalent caries, fractures, or abscesses) were noted in primary or secondary dentitions.

Case 2. A 7.11-y-old Caucasian female (subject 2) with a history of GACI and pseudoxanthoma elasticum (PXE; OMIM# 264800) presented with biallelic homozygous *ENPP1* mutations (NM_006208.2: c.1538A>G; p.Y513C in exon 15) (Fig. 1G) (Li et al. 2012). Born to consanguineous parents, she was adopted by foster parents at 3 wk of age (Fig. 1H). As part of GACI management, she was treated with bisphosphonates for 1.5 y between 5 and 7 y of age. Subject 2 had hypophosphatemia but no clinical or radiographic findings of

rickets (Appendix Table 2). Her detailed medical history is summarized in the Appendix and Appendix Figure 2E–H.

Her dental history was significant for overretained mandibular incisors, extracted at age 7 y. Oral examination revealed a normally developing mixed dentition with gingival hyperplasia (Fig. 1I; Appendix Fig. 5A–C) deemed to be associated with anticonvulsant and antihypertensive medications (e.g., levetiracetam and propranolol; see Appendix). While there was no evidence of caries, central incisors were mildly discolored (Fig. 1I, inset). Dental radiographs indicated overretained maxillary incisors (D–G) (Fig. 1J, K; Appendix Fig. 5D, E), which were extracted to provide an eruption pathway for permanent incisors. The extracted teeth exhibited a protruding root topology (Appendix Fig. 5F, G).

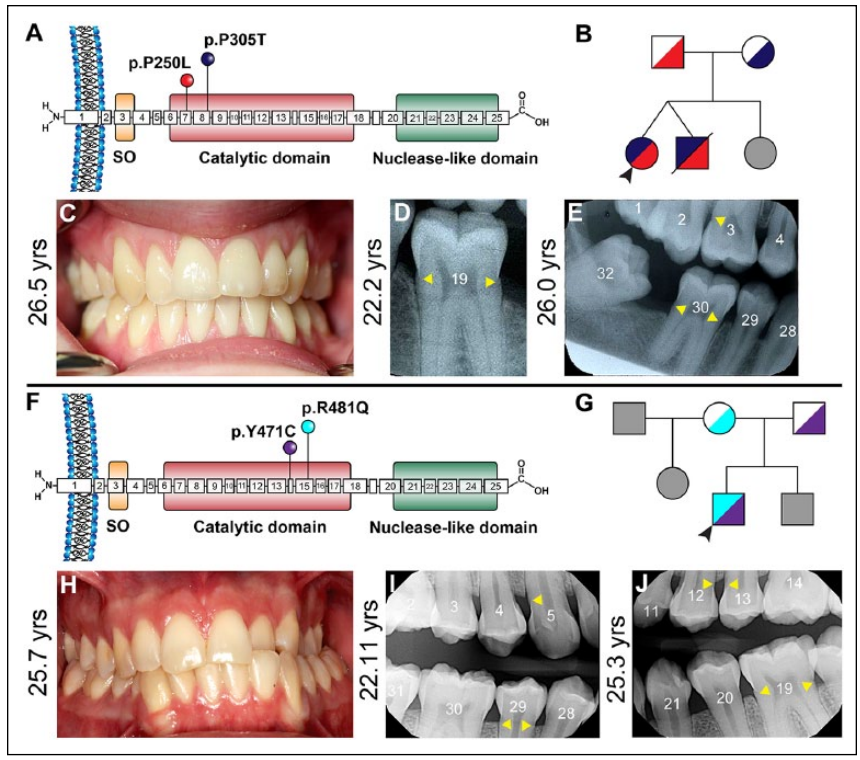

Figure 2. Clinical presentations of generalized arterial calcification of infancy (GACI) in subjects 4 and 5. (**A**) Schematic of ENPP1 protein indicating locations of p.P250L (exon 7) and p.P305T (exon 8) amino acid substitutions, both within the catalytic domain, identified in GACI subject 4. (**B**) Pedigree of proband subject 4 (black arrowhead) showing unaffected parents, twin brother who died of GACI in infancy, and unaffected younger sister (unknown genetic composition indicated by gray shading). (**C**) Oral photograph at 26.5 y reveals a healthy dentition and absence of caries, with generalized gingival recession. Dental bitewing radiographs at (**D**) 22.2 y of age and (**E**) 26.0 y show consistent protruding cervical root morphology (yellow arrowheads) in molars. (**F**) Schematic of ENPP1 protein indicating locations of p.Y471C (exon 14) and p.R481Q (exon 15) amino acid substitutions, both within the catalytic domain, identified in GACI subject 5. (**G**) Pedigree of proband subject 5 (black arrowhead) showing unaffected parents and stepfather and unaffected brother and stepsister (unknown genetic composition indicated by gray shading). (**H**) Oral photograph at 25.7 y reveals a relatively healthy dentition with unilateral crossbite and localized areas of gingival recession. Mild gingival hyperplasia is noted between maxillary central incisors. Dental bitewing radiographs at (**I**) 22.11 and (**J**) 25.3 y show consistent protruding cervical root morphology (yellow arrowheads) in posterior teeth and slightly narrow root canals in incisors.

Case 3. A 6.11-y-old Caucasian male (subject 3) with a history of GACI and Loeys-Dietz syndrome (LDS; OMIM#609192) presented with biallelic *ENPP1* mutations (NM_006208.2: c.1438T>C/p.C480R in exon 15; c.2414G>T/p.G805V in exon 23) (Fig. 1L). He is the elder of 2 children born to nonconsanguineous parents, with the father presenting with LDS and a younger sister presenting with GACI (Fig. 1M). He exhibited mild cardiovascular manifestations of GACI and was never treated with bisphosphonates. Incipient FGF23-mediated hypophosphatemic rickets was recognized at 4.2 y old (Appendix Table 2). His detailed medical history is summarized in the Appendix and Appendix Figure 2I, J.

His dental history was significant for crowding and suspected ankylosis of primary mandibular lateral incisors (N, Q), which were extracted at 6.3 y old to make space for permanent incisors (Appendix Fig. 6A, B). Oral examination revealed a normally developing mixed dentition (Fig. 1N, O). Radiographically, an unusually protruding morphology was recognized in some molar roots (Fig. 1P; Appendix Fig. 6C, D). No dental signs of hypophosphatemic rickets were noted in primary or secondary dentitions.

Case 4. Subject 4 is a 26.5-y-old Caucasian female with relatively mild cardiovascular manifestations of GACI who presented with biallelic *ENPP1* mutations (NM_006208.2: c.749C>T/p.P250L in exon 7; c.913C>A, p.P305T in exon 8) (Fig. 2A). She is 1 of 3 children born to healthy nonconsanguineous parents (Fig. 2B). A twin brother with the same *ENPP1* mutations died at 6 wk of age due to myocardial infarction. Her younger sister is reportedly healthy. No bisphosphonate treatment was administered to this subject. She was diagnosed with FGF23-mediated hypophosphatemic rickets at 8 y old (Appendix Table 2). Her detailed medical history is summarized in the Appendix and Appendix Figure 3A–C. The subject's dental history is remarkable for an infraoccluded and ankylosed primary molar (I) at 8.9 y old (Appendix Fig. 7A) and slow and difficult orthodontic treatment in her teenage years. Subject 4 presented a healthy dentition (Fig. 2C), although hypercementosis on multiple teeth was indicated in radiographs from multiple ages (Fig. 2D, E; Appendix Fig. 7B–F). A more detailed dental history is included in the Appendix.

Case 5. Subject 5 is a 25.7-y-old Caucasian male with a history of GACI who presented with biallelic mutations in *ENPP1* (NM_006208.2:c.1412A>G/p.Y471C in exon 14; c.1441C>T/p.R481W in exon 15) (Ferreira et al. 2016) (Fig. 2F). He is 1 of 3 children born to healthy nonconsanguineous parents (Fig.

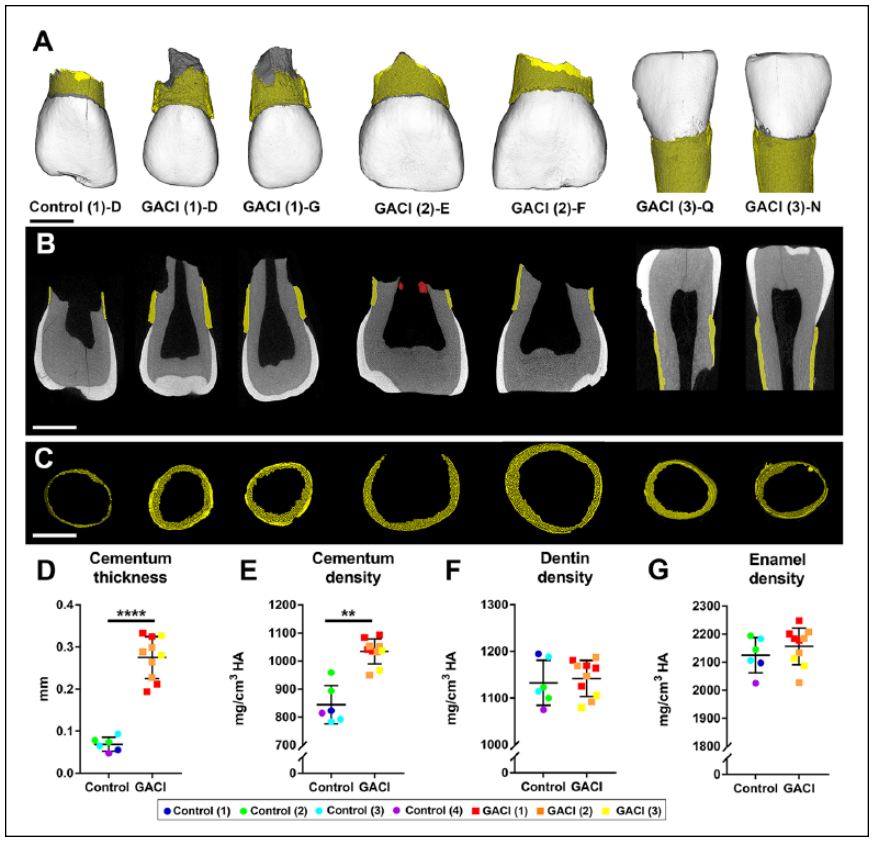

Figure 3. Increased thickness and density of cervical cementum in teeth from generalized arterial calcification of infancy (GACI) subjects. (**A**) Three-dimensional micro–computed tomography (CT) reconstructions of representative incisors from 1 healthy control and 3 GACI subjects. Cementum layer is highlighted in yellow. Scale bars in panels A to C represent 2.5 mm. (**B**) Two-dimensional micro-CT cut plane showing hypercementosis in GACI teeth. Cementum layer is highlighted in yellow. Tooth E from GACI subject 2 features calcified pulp stone-like material (labeled in red). (**C**) Segmented cervical cementum layer used for thickness measurement in control and GACI teeth. Quantitative analyses of control teeth (6 teeth from 4 subjects) and 10 GACI teeth indicate (**D**) 4-fold significantly increased cementum thickness in GACI vs. control teeth (****adjusted P = 0.00007), (**E**) 23 % increase in cementum density in GACI vs. control teeth (**adjusted P = 0.009), and no differences in (**F**) dentin density or (**G**) enamel density (adjusted $P > 0.05$ for both). In graphs shown in panels D to G, each individual tooth measurement is displayed with color coding to indicate subject of origin, with mean ± standard deviation shown for 6 teeth from n = 4 controls and 10 teeth from n = 3 GACI subjects. For independent samples t test, multiple teeth from the same individual were first averaged to compare n = 4 control and n = 3 GACI measurements, followed by Benjamini-Hochberg false discovery rate correction for Q = 0.05.

2G). His 30-y-old half-sister and 22-y-old brother are reportedly healthy. He was treated with bisphosphonates during his first 2 y and was diagnosed with FGF23-mediated hypophosphatemic rickets as a teenager (Appendix Table 2). His detailed medical history is summarized in the Appendix and Appendix Figure 3D–H. While his dental history was generally unremarkable, subject 5 presented malocclusion and crossbite (Fig. 2H). Hypercementosis was indicated in radiographs from multiple ages (Fig. 2I, J; Appendix Fig. 8). A more detailed dental history is included in the Appendix.

Hypercementosis in GACI Subjects

Ten extracted teeth from GACI subjects 1 to 3 were analyzed by high-resolution micro-CT. Teeth from subjects 4 and 5 were not available for analysis. Compared to age-matched controls (6 primary incisors from 4 subjects), GACI teeth exhibited dramatically increased cementum (Fig. 3A–C; Appendix Fig. 9). Segmentation and quantitative analysis of dental tissues revealed that GACI teeth featured 4-fold increased cementum thickness (adjusted P = 0.00007), while cementum mineral density was 23% higher (adjusted P = 0.009) than in control teeth (Fig. 3D, E). Mean enamel and dentin densities were not different between GACI and control teeth (Fig. 3F, G). Data are compiled in Appendix Table 3.

By histology, GACI teeth featured markedly increased cervical cementum compared to control teeth (Fig. 4A–F). The enlarged cementum layer in GACI teeth included cementocyte-like cells as well as empty lacunae, although this cervical region is typically acellular. While expected signs of odontoclastic/osteoclastic resorption were found in GACI primary teeth, unusual and extensive areas of reparative cementum-like material, including newly embedded cementocytes, were abundant (Fig. 4G–I). TRAP staining identified osteoclasts/odontoclasts on actively resorbing root surfaces, but TRAP-positive cells were absent from surfaces showing reparative cementum-like material covering resorbed edges (Appendix Fig. 10). Picrosirius red staining observed with polarized light microscopy demonstrated inclusion of densely packed, normally oriented Sharpey's fibers in the thick cementum of GACI teeth, confirming it as extrinsic fiber cementum (Appendix Fig. 11). IHC revealed selectively localized ENPP1 expression in cementoblasts lining the root surfaces of control human and mouse teeth (Fig. 4J–M).

Hypercementosis in Enpp1 *Mutant Mouse Model of GACI*

Enpp1 loss-of-function mice feature decreased PP_i concentrations, hypermineralization, vascular calcification consistent with that in GACI patients, and FGF23-driven hypophosphatemic rickets (Harmey et al. 2004; Mackenzie et al. 2012; Li et al. 2013). We previously reported histological findings from *Enpp1* loss-of-function mouse models (Nociti et al. 2002; Foster et al. 2012; Zweifler et al. 2015) and here analyzed *Enpp1*$^{asj/asj}$ and WT mouse mandibular molars by high-resolution micro-CT in parallel to human teeth (Fig. 5). Compared to WT,

Enpp1$^{asj/asj}$ molars exhibited 4-fold increased cervical cementum thickness (adjusted $P = 0.002$), 5-fold increased volume (adjusted $P = 0.002$), and a 5% nonsignificant increase in mineral density (Fig. 5A–G). Apically located cellular cementum showed significantly increased volume (50%; adjusted $P = 0.02$) and height on mesial root surface (35%; adjusted $P = 0.01$) but no change in thickness or density in *Enpp1*$^{asj/asj}$ versus WT mice (Fig. 5H–L). No other linear, volumetric, or density measurements of dental tissues were different between *Enpp1*$^{asj/asj}$ versus WT mice (Appendix Fig. 12). Histology of *Enpp1*$^{asj/asj}$ mouse molars resembled that of GACI subjects, including dramatically expanded cervical cementum with abnormal inclusion of embedded cells and lacunae (Appendix Fig. 13).

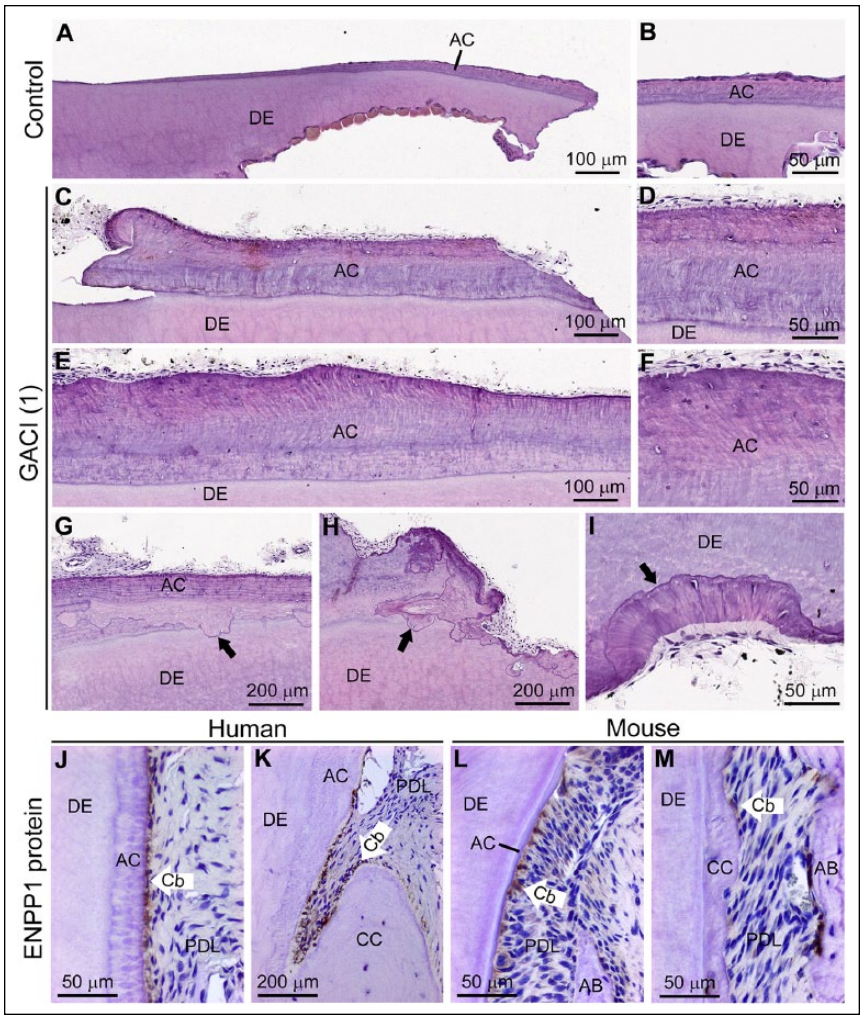

Figure 4. Histological analysis of hypercementosis in teeth from generalized arterial calcification of infancy (GACI) subjects. Histology sections of (**A, B**) healthy control incisor compared to (**C, D**) incisor and (**E, F**) canine from GACI subject 1 reveal dramatically increased acellular cementum (AC) in GACI teeth. Both GACI teeth exhibit embedded nucleated cementocyte-like cells and empty lacunae (D and F) unusual for cervical cementum. (**G–I**) GACI teeth exhibit patterns of adjacent resorption and reparative cellular cementum (black arrows), unusual for primary teeth undergoing exfoliation. Immunohistochemistry for ENPP1 protein in control (**J, K**) human and (**L, M**) mouse molar sections reveals selective elevated ENPP1 in cementoblasts (Cb) lining AC surfaces, with fewer positive Cb on the cellular cementum (CC) surfaces. AB, alveolar bone; DE, dentin; PDL, periodontal ligament.

Discussion

We report for the first time dental manifestations of inactivating *ENPP1* mutations in 5 individuals with GACI, all presenting significant hypercementosis of cervical cementum in primary and/or secondary dentition. Similar to GACI subjects, *Enpp1*$^{asj/asj}$ mice exhibited significant hypercementosis. Dental histories of 4 GACI subjects included evidence for infraocclusion, overretained primary teeth, possible ankylosis, and/or ineffective orthodontic tooth movement, suggesting altered mineral metabolism contributing to disrupted tooth movement and exfoliation. While 4 of 5 GACI subjects presented with signs of hypophosphatemic rickets, associated deleterious effects on dental tissues were not evident. Immunolocalization of ENPP1 in human and mouse cementoblasts supports a specific role for this protein in controlling cementogenesis. Collectively, these findings illustrate a novel dental phenotype in GACI and *ENPP1* mutations associated with hypercementosis. The sensitivity of cementum to reduced PP_i levels in both human and mouse teeth establishes this mechanism as a well-conserved and fundamental biological process directing cementogenesis across species.

Influence of Pyrophosphate on Cementogenesis

ENPP1 is a membrane-bound enzyme of the ectonucleotide pyrophosphatase/phosphodiesterase family (Stefan et al. 2005) expressed by osteoblasts and chondrocytes, which contributes to regulation of skeletal mineralization (Millán 2013). ENPP1 generates intracellular/extracellular PP_i by hydrolyzing ATP to AMP and PP_i. ENPP1-derived PP_i is critical for preventing pathological soft tissue calcification, and decreased PP_i levels account for GACI-associated pathologic calcifications (Rutsch et al. 2003; Ferreira et al. 2014). We reported previously that extracellular PP_i deficiency in *Enpp1* mutant and knockout mice contributes to increased acellular cementum formation (Nociti et al. 2002; Foster et al. 2012). A nearly identical cementum phenotype is noted in mice with loss of function of ANK, a transmembrane protein that mediates transport of intracellular PP_i to the extracellular space (Nociti et al. 2002; Foster et al. 2012). However, to date, it remained unclear if the role of ENPP1 in tooth development is conserved between

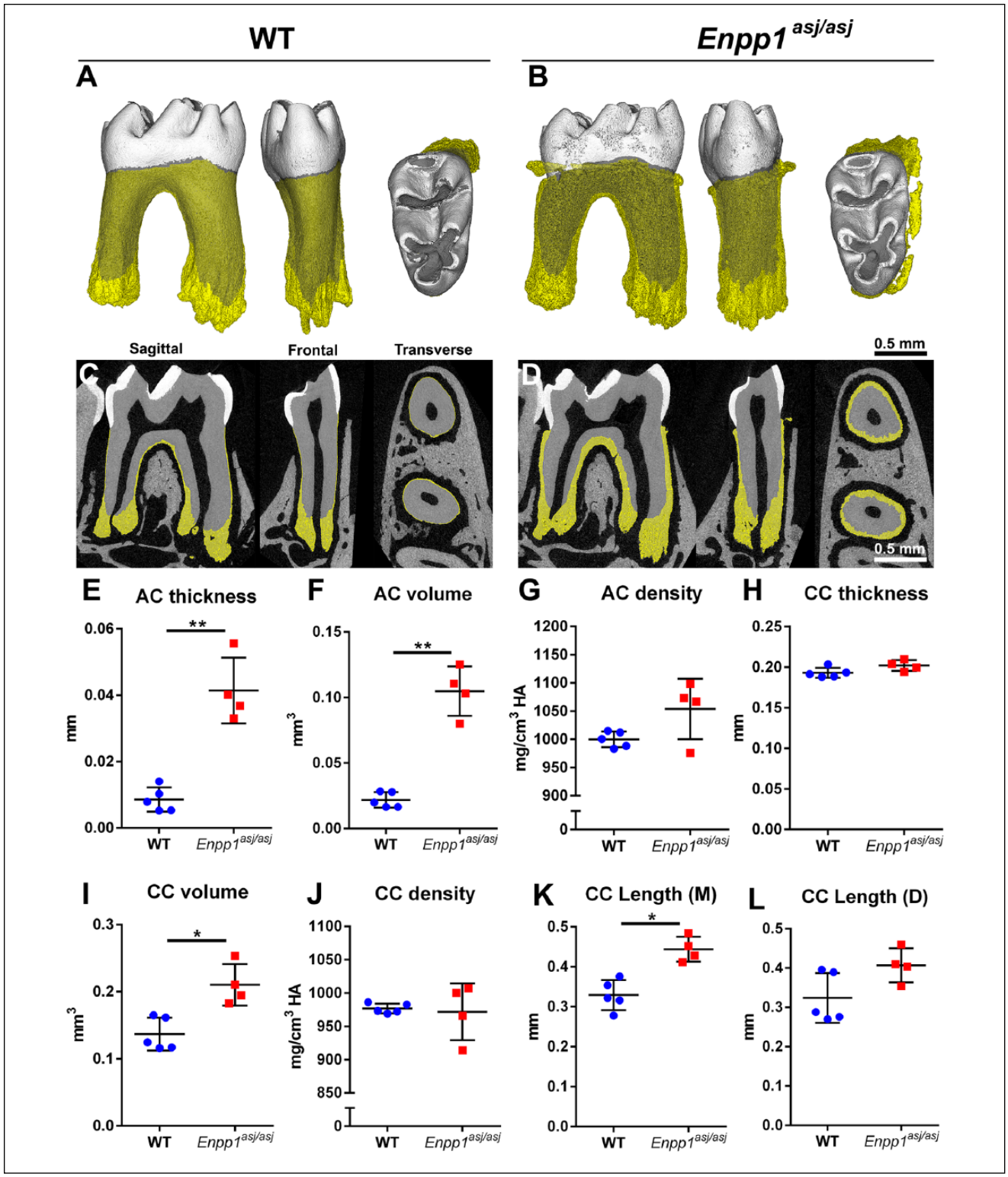

Figure 5. *Enpp1* mutant mice feature increased acellular and cellular cementum dimensions. High-resolution micro–computed tomography analysis reveals hypercementosis in *Enpp1*$^{asj/asj}$ versus wild-type (WT) mouse first mandibular molars (n = 4 to 5) in (**A, B**) 3-dimensional reconstructions and (**C, D**) 2-dimensional cut planes in sagittal, frontal, and transverse orientations. Cementum layer is highlighted in yellow. Quantitative analysis of molars shows significantly increased (**E**) acellular cementum (AC) thickness (**adjusted P = 0.002) and (**F**) volume (**adjusted P = 0.002), and (**G**) a nonsignificant increase in mean AC density in *Enpp1*$^{asj/asj}$ versus WT mice. (**H–L**) Significant increases are observed in cellular cementum (CC) volume (*adjusted P = 0.02) and length on mesial (M) root (*adjusted P = 0.01), although differences are not found in thickness, density, or distal (D) root CC length (adjusted P > 0.05 for all). For independent samples t test, calculated P values were adjusted and statistical significance determined by the Benjamini-Hochberg procedure for Q = 0.05.

mouse and human, as key differences between the 2 include extremely rapid tooth formation in mice (weeks rather than years) and formation of only a single dentition in mice. It has also been unclear whether different proteins exert more dominant influences on cementogenesis in different species. Our results indicate that hypercementosis of cervical cementum from *ENPP1* loss of function is consistent in humans and mice. Bisphosphonates affect bone remodeling and have been linked to altered/ectopic bone deposition and so might be suspected in hypercementosis. However, it is important to note that cementum does not undergo physiological remodeling, and bisphosphonate administration to rodents inhibits acellular cementum formation (Beertsen et al. 1985). Furthermore, GACI subjects 3 and 4 and *Enpp1*$^{asj/asj}$ mice all featured hypercementosis without bisphosphonate treatment.

ENPP1 immunolocalization in cementoblasts of both mouse and human teeth supports its role as a regulator of cementum growth under physiological circumstances through local production of PP_i. However, while previous studies support a local role for ENPP1 and PP_i in directing mineralization (Anderson et al. 2005; Foster et al. 2012), we cannot rule out the influence of systemic factors based on these data. In contrast to ENPP1, TNAP reduces PP_i and loss-of-function mutations in *ALPL* cause HPP, a disorder where elevated PP_i causes skeletal hypomineralization (Whyte 2016) and acellular cementum aplasia or hypoplasia (Foster, Ramnitz, et al. 2014b), the exact opposite effect of hypercementosis noted in GACI subjects with pathologically low PP_i.

Additional Dental Manifestations of GACI

Individuals with GACI who survive infancy may develop autosomal recessive hypophosphatemic rickets type 2 (ARHR2; OMIM#613312) within the first decade of life. ARHR2 is characterized by elevated FGF23, decreased serum phosphate, decreased renal phosphate reabsorption, and elevated serum alkaline phosphatase (Rutsch et al. 2008; Levy-Litan et al. 2010; Lorenz-Depiereux et al. 2010; Ferreira et al. 2016). The etiology of ARHR2 is unclear. Onset of ARHR2 can be as early as 1 y old, and primary and secondary teeth during this stage are sensitive to mineral disturbances as evidenced by other forms of nutritional and inherited rickets, for example, X-linked hypophosphatemia (XLH; OMIM#307800) and vitamin D–dependent rickets (VDDR1A; OMIM#264700) (Davit-Beal et al. 2014; Biosse Duplan et al. 2016). These metabolic disturbances cause severe enamel and dentin defects, making teeth susceptible to caries, fractures, and abscesses. Four GACI subjects described in this study showed skeletal and biochemical signs of ARHR2 (Appendix Table 2; Appendix Fig. 2). However, subjects 1 to 4 showed no signs of rachitic dental manifestations. Subject 5 presented unusual cusp patterns and a history of extensive sealant application, as noted previously (Ferreira et al. 2016). While these observations are consistent with very mild enamel effects, in isolation they are not strong evidence of rachitic teeth. Administration of bisphosphonates in infancy could also plausibly disturb dental mineralization based on prior reports in humans and rodents (Bradaschia-Correa et al. 2007; Hiraga et al. 2010; Iwai et al. 2013; Soares et al. 2016).

Primary molars were infraoccluded in subjects 1 and 4, in addition to atypical infraocclusion of primary incisors in subject 1. Subject 2 presented failure of natural exfoliation of primary incisors. Etiology of infraocclusion is difficult to determine, with hypotheses including ankylosis, impaction, absence of successor, damage to developing root, bone defects, and metabolic disturbances (Noble et al. 2007). Mandibular first primary molars are reportedly the most commonly affected teeth (McGeown and O'Connell 2014) with no existing reports of infraoccluded anterior teeth. Ankylosis might be suspected due to altered periodontal mineralization but was not identified in retained teeth in subjects 1 and 2, although it was indicated in mandibular primary incisors in subject 3 and the infraoccluded primary molar in subject 4. Substantial root structure remained on teeth from subjects 1 (extracted at 8 y old) and 3 (extracted at 6 y old) compared to healthy controls, and there was histological evidence of extensive repair cementum in teeth from subject 1, suggesting that new cementum formation could have been opposing and reversing odontoclast activities. Altered resorption may also be suspected. While defective osteoclast/odontoclast resorption has not been linked to *ENPP1* in humans or animal models (Hajjawi et al. 2014), loss of function of ANK/ANKH contributes to osteoclast dysfunction in craniometaphyseal dysplasia (Chen et al. 2014). Intriguingly, orthodontic records for subject 4 report difficulty in orthodontic tooth movement, suggesting reduced bone resorption. Another hypothesis for infraocclusion arises from bisphosphonate treatment, a life-saving intervention that may have unintended consequences on skeletal and dental tissues (Rutsch et al. 2008; Edouard et al. 2011; Otero et al. 2013; Soares et al. 2016). Bisphosphonate administration in animals disrupted tooth eruption (Grier and Wise 1998; Bradaschia-Correa et al. 2007; Hiraga et al. 2010) and was associated with delayed eruption in humans (Kamoun-Goldrat et al. 2008; Iwai et al. 2013). However, subject 4, who experienced both infraocclusion and slow orthodontic tooth movement, was never treated with bisphosphonates, suggesting that *ENPP1* mutations are responsible. Strikingly, a previous report of familial hypercementosis noted infraocclusion of several molars and premolars, recalcitrance to orthodontic tooth movement, and abnormal deposition of cementum layers over resorption lacunae (Humerfelt and Reitan 1966). These and other findings in human subjects warrant further studies to elucidate underlying mechanisms.

Author Contributions

V. Thumbigere-Math, B.L. Foster, contributed to conception, design, data acquisition, analysis, and interpretation, drafted and critically revised the manuscript; A. Alqadi, C.R. Ferreira, K. FitzGerald, contributed to conception, design, data acquisition, analysis, and interpretation, critically revised the manuscript; N.I. Chalmers, contributed to data acquisition, critically revised the manuscript; M.B. Chavez, contributed to data analysis and interpretation, critically revised the manuscript; E.Y. Chu, M.T.

Collins, R.I. Gafni, W.A. Gahl, K.S. Hsu, M.S. Ramnitz, S.G. Ziegler, contributed to data acquisition, analysis, and interpretation, critically revised the manuscript; M.J. Somerman, contributed to conception, design, data analysis, and interpretation. All authors gave final approval and agree to be accountable for all aspects of the work.

Acknowledgments

We thank the subjects and their families for their cooperation and assistance with this research. We thank Dr. Janice Lee and Dr. Pamela Gardner (National Institute of Dental and Craniofacial Research [NIDCR]/National Institutes of Health [NIH]) for helping facilitate this research study. We thank Dr. Nathaniel Cook for arranging sample shipment and Dr. Joshua Spiegl, Dr. Mona Beylin, and Dr. James A. Jespersen for providing dental records. We thank Dr. Kristina Zaal (Light Imaging Section, National Institute of Arthritis and Musculoskeletal and Skin Diseases [NIAMS]/NIH) for assistance in slide scanning and Alyssa Coulter (NIAMS/NIH) for assistance with histological sectioning. We thank Dr. Heidi Steinkamp (College of Dentistry, The Ohio State University) for assistance in tooth identification. This research was supported by grants AR 066110 to BLF and AR 069643 to VTM from NIAMS, NIH, Bethesda, MD, and intramural funding from NIDCR/NIH (to RIG and MSR), NIAMS/NIH (to MJS), and National Human Genome Research Institute (NHGRI)/NIH (to CRF and WAG). The authors declare no potential conflicts of interest with respect to the authorship and/or publication of this article.

References

Anderson H, Harmey D, Camacho N, Garimella R, Sipe J, Tague S, Bi X, Johnson K, Terkeltaub R, Millán J. 2005. Sustained osteomalacia of long bones despite major improvement in other hypophosphatasia-related mineral deficits in tissue nonspecific alkaline phosphatase/nucleotide pyrophosphatase phosphodiesterase 1 double-deficient mice. Am J Pathol. 166(6):1711–1720.

Beertsen W, Niehof A, Everts V. 1985. Effects of 1-hydroxyethylidene-1, 1-bisphosphonate (HEBP) on the formation of dentin and the periodontal attachment apparatus in the mouse. Am J Anat. 174(1):83–103.

Biosse Duplan M, Coyac BR, Bardet C, Zadikian C, Rothenbuhler A, Kamenicky P, Briot K, Linglart A, Chaussain C. 2017. Phosphate and vitamin D prevent periodontitis in X-linked hypophosphatemia. J Dent Res. 96(4):388–395.

Bradaschia-Correa V, Massa LF, Arana-Chavez VE. 2007. Effects of alendronate on tooth eruption and molar root formation in young growing rats. Cell Tissue Res. 330(3):475–485.

Chen IP, Tadinada A, Dutra EH, Utreja A, Uribe F, Reichenberger EJ. 2014. Dental anomalies associated with craniometaphyseal dysplasia. J Dent Res. 93(6):553–558.

Davit-Beal T, Gabay J, Antoniolli P, Masle-Farquhar J, Wolikow M. 2014. Dental complications of rickets in early childhood: case report on 2 young girls. Pediatrics. 133(4):e1077–e1081.

Edouard T, Chabot G, Miro J, Buhas DC, Nitschke Y, Lapierre C, Rutsch F, Alos N. 2011. Efficacy and safety of 2-year etidronate treatment in a child with generalized arterial calcification of infancy. Eur J Pediatr. 170(12):1585–1590.

Ferreira C, Ziegler S, Gahl W. 2014. Generalized arterial calcification of infancy. In: Pagon RA, Adam MP, Ardinger HH, Wallace SE, Amemiya A, Bean LJH, Bird TD, Fong CT, Mefford HC, Smith RJH, et al., editors. Genereviews(r). Seattle: University of Washington.

Ferreira CR, Ziegler SG, Gupta A, Groden C, Hsu KS, Gahl WA. 2016. Treatment of hypophosphatemic rickets in generalized arterial calcification of infancy (GACI) without worsening of vascular calcification. Am J Med Genet A. 170A(5):1308–1311.

Foster BL. 2012. Methods for studying tooth root cementum by light microscopy. Int J Oral Sci. 4(3):119–128.

Foster BL, Kuss P, Yadav MC, Kolli TN, Narisawa S, Lukashova L, Cory E, Sah RL, Somerman MJ, Millan JL. 2017. Conditional alpl ablation phenocopies dental defects of hypophosphatasia. J Dent Res. 96(1):81–91.

Foster BL, Nagatomo KJ, Nociti FH, Fong H, Dunn D, Tran AB, Wang W, Narisawa S, Millán JL, Somerman MJ. 2012. Central role of pyrophosphate in acellular cementum formation. PLoS One. 7(6):e38393.

Foster BL, Nociti FH Jr, Somerman MJ. 2014. The rachitic tooth. Endocr Rev. 35(1):1–34.

Foster BL, Ramnitz MS, Gafni RI, Burke AB, Boyce AM, Lee JS, Wright JT, Akintoye SO, Somerman MJ, Collins MT. 2014. Rare bone diseases and their dental, oral, and craniofacial manifestations. J Dent Res. 93(7 Suppl):7S–19S.

Foster BL, Somerman MJ. 2012. Cementum. In: McCauley LK, Somerman MJ, editors. Mineralized tissues in oral and craniofacial science: biological principles and clinical correlates. Ames (IA): Wiley-Blackwell. p. 169–192.

Grier RL IV, Wise GE. 1998. Inhibition of tooth eruption in the rat by a bisphosphonate. J Dent Res. 77(1):8–15.

Hajjawi MO, MacRae VE, Huesa C, Boyde A, Millan JL, Arnett TR, Orriss IR. 2014. Mineralisation of collagen rich soft tissues and osteocyte lacunae in Enpp1(–/–) mice. Bone. 69:139–147.

Harmey D, Hessle L, Narisawa S, Johnson K, Terkeltaub R, Millán J. 2004. Concerted regulation of inorganic pyrophosphate and osteopontin by akp2, enpp1, and ank: an integrated model of the pathogenesis of mineralization disorders. Am J Pathol. 164(4):1199–1209.

Hiraga T, Ninomiya T, Hosoya A, Nakamura H. 2010. Administration of the bisphosphonate zoledronic acid during tooth development inhibits tooth eruption and formation and induces dental abnormalities in rats. Calcif Tissue Int. 86(6):502–510.

Humerfelt A, Reitan K. 1966. Effects of hypercementosis on the movability of teeth during orthodontic treatment. Angle Orthod. 36(3):179–189.

Iwai T, Isomatsu Y, Iwamoto M, Tohnai I. 2013. Bisphosphonate-related enamel hypoplasia in a child with idiopathic arterial calcification of infancy. Br J Oral Maxillofac Surg. 51(7):e186–e187.

Kamoun-Goldrat A, Ginisty D, Le Merrer M. 2008. Effects of bisphosphonates on tooth eruption in children with osteogenesis imperfecta. Eur J Oral Sci. 116(3):195–198.

Levy-Litan V, Hershkovitz E, Avizov L, Leventhal N, Bercovich D, Chalifa-Caspi V, Manor E, Buriakovsky S, Hadad Y, Goding J, et al. 2010. Autosomal-recessive hypophosphatemic rickets is associated with an inactivation mutation in the ENPP1 gene. Am J Hum Genet. 86(2):273–278.

Li Q, Guo H, Chou DW, Berndt A, Sundberg JP, Uitto J. 2013. Mutant Enpp1asj mice as a model for generalized arterial calcification of infancy. Dis Model Mech. 6(5):1227–1235.

Li Q, Schumacher W, Jablonski D, Siegel D, Uitto J. 2012. Cutaneous features of pseudoxanthoma elasticum in a patient with generalized arterial calcification of infancy due to a homozygous missense mutation in the ENPP1 gene. Br J Dermatol. 166(5):1107–1111.

Lorenz-Depiereux B, Schnabel D, Tiosano D, Häusler G, Strom T. 2010. Loss-of-function ENPP1 mutations cause both generalized arterial calcification of infancy and autosomal-recessive hypophosphatemic rickets. Am J Hum Genet. 86(2):267–272.

Mackenzie NC, Zhu D, Milne EM, van't Hof R, Martin A, Quarles DL, Millán JL, Farquharson C, MacRae VE. 2012. Altered bone development and an increase in FGF-23 expression in Enpp1(–/–) mice. PLoS One. 7(2):e32177.

McGeown M, O'Connell A. 2014. Management of primary molar infraocclusion in general practice. J Ir Dent Assoc. 60(4):192–198.

Millán JL. 2013. The role of phosphatases in the initiation of skeletal mineralization. Calcif Tissue Int. 93(4):299–306.

Noble J, Karaiskos N, Wiltshire WA. 2007. Diagnosis and management of the infraerupted primary molar. Br Dent J. 203(11):632–634.

Nociti FH Jr, Berry JE, Foster BL, Gurley KA, Kingsley DM, Takata T, Miyauchi M, Somerman MJ. 2002. Cementum: a phosphate-sensitive tissue. J Dent Res. 81(12):817–821.

Opsahl Vital S, Gaucher C, Bardet C, Rowe PS, George A, Linglart A, Chaussain C. 2012. Tooth dentin defects reflect genetic disorders affecting bone mineralization. Bone. 50(4):989–997.

Otero JE, Gottesman GS, McAlister WH, Mumm S, Madson KL, Kiffer-Moreira T, Sheen C, Millan JL, Ericson KL, Whyte MP. 2013. Severe skeletal toxicity from protracted etidronate therapy for generalized arterial calcification of infancy. J Bone Miner Res. 28(2):419–430.

Reibel A, Manière M, Clauss F, Droz D, Alembik Y, Mornet E, Bloch-Zupan A. 2009. Orodental phenotype and genotype findings in all subtypes of hypophosphatasia. Orphanet J Rare Dis. 4:6.

Rutsch F, Böyer P, Nitschke Y, Ruf N, Lorenz-Depierieux B, Wittkampf T, Weissen-Plenz G, Fischer R, Mughal Z, Gregory J, et al. 2008. Hypophosphatemia, hyperphosphaturia, and bisphosphonate treatment are associated with survival beyond infancy in generalized arterial calcification of infancy. Circ Cardiovasc Genet. 1(2):133–140.

Rutsch F, Ruf N, Vaingankar S, Toliat M, Suk A, Höhne W, Schauer G, Lehmann M, Roscioli T, Schnabel D, et al. 2003. Mutations in ENPP1 are associated with 'idiopathic' infantile arterial calcification. Nat Genet. 34(4):379–381.

Soares AP, do Espirito Santo RF, Line SR, Pinto M, Santos Pde M, Toralles MB, do Espirito Santo AR. 2016. Bisphosphonates: pharmacokinetics, bioavailability, mechanisms of action, clinical applications in children, and effects on tooth development. Environ Toxicol Pharmacol. 42: 212–217.

Stefan C, Jansen S, Bollen M. 2005. NPP-type ectophosphodiesterases: unity in diversity. Trends Biochem Sci. 30(10):542–550.

Whyte MP. 2016. Hypophosphatasia—aetiology, nosology, pathogenesis, diagnosis and treatment. Nat Rev Endocrinol. 12(4):233–246.

Zweifler LE, Patel MK, Nociti FH Jr, Wimer HF, Millan JL, Somerman MJ, Foster BL. 2015. Counter-regulatory phosphatases TNAP and NPP1 temporally regulate tooth root cementogenesis. Int J Oral Sci. 7(1):27–41.